Materials Research. 2018; 21(1): e20170148
DOI: http://dx.doi.org/10.1590/1980-5373-MR-2017-0148

Corrosion Behavior of Duplex and Lean Duplex Stainless Steels in Pulp Mill

Luiza Esteves[a]*, Marcelo Cardoso[a], Vanessa de Freitas Cunha Lins[a]

[a]Departamento de Engenharia Química, Universidade Federal de Minas Gerais, Av. Pres. Antônio Carlos, 6627, Cep. 31270-901, Pampulha, Belo Horizonte, MG, Brazil

Received: January 18, 2017; Revised: October 16, 2017; Accepted: November 10, 2017

The cyclic potentiodynamic polarization behavior of duplex stainless steel (DSS) and lean duplexstainless steel (LDSS) was studied in white and green liquors froma pulp processingplant. The corrosion behavior in industrial and also synthetic liquor was compared. The polarization curves of the duplex steels in synthetic white liquor were shifted to lower potentials and higher current densities in relation to the steel in industrial white liquor, which proved to be less aggressive to the duplex steel. The duplex steels also showed the highest values of transpassive potential in industrial white liquor compared to synthetic liquor. Cold and hot rolled duplex and lean duplex steels in green liquor showed the lowest values of transpassive potential.

Keywords: *Duplex stainless steels, Polarization, Alkaline corrosion, Pulp and paper industry.*

1. Introduction

Chemical pulps are made by cooking (digesting) the raw materials, using the Kraft process (sulfate) and sulfite processes. The Kraft process is the most dominating chemical pulping process worldwide. In the Kraft pulp process, the active cooking chemicals (white liquor) are mainly sodium hydroxide (NaOH) and sodium sulfide (Na_2S)[1,2], the operation is at high temperature (about 170 ºC) and the pressure of 6.5 to 8.5 bar is used in delignification during the chip cooking cycle[3-5]. The chemical recovery cycle is generated the sub-product, extracted from pulping wood in the digester, called the black liquor, with smaller amounts of wood extractives and residual inorganic pulping salt[6,7]. The combustion of the strong black liquor converts the recovered inorganic chemicals to smelt which is dissolved in water to give the green liquor, which are mainly sodium carbonate (Na_2CO_3), and sodium sulfide (Na_2S) generated during the liquor recovery cycle. The green liquor is causticized to regenerate the white liquor[8-13]. The scheme of the main operation of the chemical recovery cycle is shown in Figure 1. Moreover, the white liquor is considered the most aggressive of the alkaline pulping liquors[14].

Duplex stainless steel (DSS) has been used as a material of construction in the pulp and paper industry for the past 35 years due to its excellent corrosion resistance and high mechanical strength allowing for thickness reduction in equipment. Lean DSS (LDSS) is a DSS with a lower content of molybdenum and nickel and thus a lower cost. Nitrogen addition is used in LDSS to provide the austenite content in alloys with a lower nickel concentration[15-17]. Currently, the materials commonly selected for the construction of pulp digesters are lean duplex (UNS S32304) or standard duplex (UNS S32205). Older facilities were constructed from AISI 316 austenitic stainless steel coupled to an anodic protection system[18-22]. DSSs combine low nickel content with high mechanical strength, which makes them an efficient and cost alternative to austenitic stainless steel grades.

In the pulp and paper industry, carbon steel pulp mill equipment, like digesters, storage vessels, have been showed general corrosion and stress corrosion cracking[14,23-25]. Singh and Anaya evaluated the corrosion behavior of carbon steel (A 516-Gr 70), AISI 304 and 316 stainless steels, and two DSSs (UNS S32304, UNS S32205) in black liquor produced by pulping five wood species in a synthetic liquor. The potentiodynamic polarization tests were performed at room temperature, with and without the addition of catechols. The organic compounds in the black liquor were found to play a major role in steel corrosion, and the DSSs showed a high corrosion resistance in all tested black liquors[22].

Corrosion resistance of DSS in white liquor has been widely studied[14,21-23]. The corrosion properties and electrochemical behavior of different DSSs (UNS S32304, UNS S32205, and UNS S32101) in high pH caustic and alkaline sulfide solutions at different temperatures were investigated by Bhattacharya and Singh[14]. They studied the role of alloying elements in DSS in these environments by analyzing the polarization behavior of pure Fe, Cr, Ni and Mo, and DSS UNS S32205. The increase in corrosion rates of DSS with sulfide addition can be related to the presence of sulfur in the passive layer and the formation of metal-sulfur compounds thatare less protective than the oxide film[14]. The S32205 steel was found to be most susceptible to general corrosion and the S32304 steel had the lowest corrosion rates in a sulfide caustic environment. A more stable passive film containing magnetite and awaruite ($FeNi_3$) developed on UNS S32304 steel, resulting in lower corrosion rates[14].

*e-mail: luizaeq@yahoo.com.br

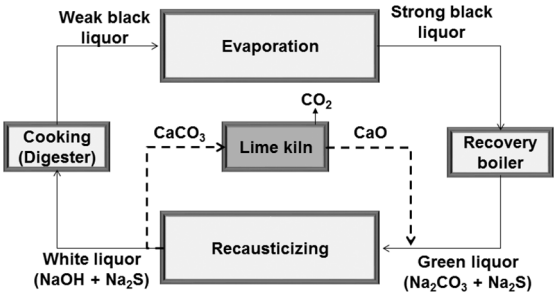

Figure 1. Schematic representation of the paper and pulp mill (Kraft process).

Wensley and Champagne[26] evaluated the effect of sulfide concentration on the corrosion resistance of carbon steel specimens with different silicon contents (low-silicon A285-Grade C and medium-silicon A516-Grade 70), austenitic stainless steel (ASI04) and two DSS (UNS S32304 and UNS S32205) in white, green, weak black, strong black, and flash tank liquors. All of the stainless steels (UNS S30403, UNS S32304, and UNS S32205) were highly resistant to corrosion in all the liquors tested, regardless of sulfide content[23,26,27].

The aim of this work is to evaluate the corrosion behavior of DSS with two processing conditions, hot and cold rolling in liquors provided by a pulp and paper industry. Also, the corrosion resistance of DSS and LDSS in synthetic and industrial white liquor (WL) is compared. To the best of our knowledge, literature on corrosion behavior of LDSS and DSS in industrial liquors from pulp and paper industry is not reported and the mechanisms involved are not fully understood.

2. Materials and Methods

The duplex stainless steels were supplied by Aperam South America (Brazil) in hot rolled and cold rolled conditions and the chemical compositions of the steels are shown in Table 1. The DSS studied is 31803 with 5%wt. Ni and 2.6%wt. Mo and the LDSS is 32304 with a lower content of Ni (4%wt.) and Mo (0.3%wt.). The steels were examined as-received: hot rolled coils annealed at 1075 ± 25ºC with a thickness of 4 mm, and cold rolled coils annealed at 1070 ± 25 ºC, with a thickness of 1.8 mm. Table 2 shows the mechanical properties of the cold rolled and hot rolled steels provided by the manufacturer[28].

The metallographic analysis was performedafter etching the steel samples in modified Behara reagent [80 mL distilled and deionized water, 20 mL hydrochloric acid (HCl), and 1 g of potassium metabisulfite ($K_2S_2O_5$)]; 2 g of ammonium bifluoride (NH_4H HF) were added to this stock solution just before the etching[29]. The microstructure analyses were carried out using an optical light microscope (LOM, Leitz Metalloplan) with Image Pro software.

The steel sheets were cut in dimensions of 1 cm x 1 cm with the exposed surface being the rolling surface. The samples were embedded in epoxy resin and electrical connections necessary for the tests were made by welding a copper wire tothe back of the sample, which was not in contact with the electrolyte. The samples were wet ground to 1200 grit SiC abrasive papers, and then polished using 3 µm, 1 µm, and 0.25 µm diamond paste, and ultrasonically cleaned in ethanol. In order to avoid crevices, the samples were masked with black wax (Apiezon Wax W)[30] at least 12 h before testing and were stored in a desiccator. The black wax was dissolved in trichloroethylene to assist application.

The white and green liquors were supplied by a North American pulp and paper company. The WL contained sodium hydroxide (NaOH) and sodium sulfide (Na_2S) at pH > 13, the green liquor (GL) aqueous solution contained sodium carbonate (Na_2CO_3) and sodium sulfide (Na_2S) at pH >10. The electrochemical tests were also performed in synthetic white liquor (SWL) composed of 150 g/L of NaOH and 153.8 g/L of $Na_2S.9H_2O$ (3.75 mol/L NaOH + 0.64 mol/L Na_2S)[14,31].

All sodium components were considered on the basis of the equivalent amount of sodium oxide (Na_2O). The definitions used were based on the Technical Association of Pulp and Paper industries (TAPPI). The effective alkali (EA) is: NaOH +1/2 Na_2S, expressed as Na_2O; the total alkali is NaOH + Na_2S + Na_2CO_3 + 1/2 Na_2CO_3, all expressed as Na_2O[22]. The sulphide-containing caustic solutions used were: WL consisting of 88 g/L EA as Na_2O and GL consisting of 117g/L total titratable alkali (TTA) as Na_2O. The GL and WL were originated by pulping of pine mix and hardwood mix.

A Reference 600 Gamry potentiostat was used for the electrochemical tests. The polarization curves were collected by scanning to the anodic direction at 0.167 mV/s from the corrosion potential (E_{corr}). Transpassivity was observed in all cases, and the scan was reversed when the current reached

Table 1. Chemical composition of the DSSs investigated (wt%).

Steel	Rolling	Cr	Ni	Mo	N	C	Si	Mn	S
31803	**Cold**	22.43	5.34	2.67	0.11	0.012	0.29	1.85	0.0004
31803	**Hot**	22.45	5.31	2.63	0.11	0.013	0.38	1.81	0.0005
32304	**Cold**	22.40	4.10	0.29	0.14	0.015	0.46	1.55	0.0002
32304	**Hot**	22.87	4.20	0.27	0.15	0.011	0.20	1.45	0.0004

Table 2. Mechanical properties of duplex steels.

Steel samples	Hardness (Rockwell C)	Elongation (%)	Yield Strength (MPa)	Tensile strength (MPa)
DSS Cold rolled S31803	23	28	700	855
DSS Hot rolled S31803	22	30	648	784
LDSS Cold rolled S32304	19	31	604	764
LDSS Hot rolled S32304	18	33	557	691

3 mA/cm^2. All the electrochemical measurements were repeated at least three times to ensure the reproducibility.

Potentiostatic polarization was performed in GL to evaluate the efficiency of the protective layer. Three potential values were chosen for the potentiostatic tests: -500 mV_{SCE} at the first passivation (around 10^{-6} A/cm^2), -150 mV_{SCE} at the second passivation (around 10^{-5} A/cm^2), and 0 mV_{SCE} in the transpassive region.

3. Results and Discussion

3.1 Steel characterization

The microstructure of the two steels, DSS and LDSS are shown in Figure 2. Lighter austenite (γ) islands are embedded in the darkeretched ferrite (α) matrix with no other secondary precipitates[32,33]. The cold rolled condition of the steels showed higher yield strength, a higher tensile strength, and a lower elongation than the hot rolled condition of the steels, even though the steels were annealed at 1070 ± 25ºC after rolling. Table 3 shows the contents of austenite and ferrite obtained using Image Pro Software.

Table 3. Austenite and ferrite contents obtained using Image Pro Software.

Samples	Weight percent	
	Austenite (γ)	Ferrite (Fe-α)
DSS 31803 Cold Rolled	48	52
DSS 31803 Hot Rolled	50	50
LDSS 32304 Cold Rolled	47	53
LDSS 32304 Hot Rolled	46	54

3.2 Cyclic polarization of DSS S31803 and S32304 steels in synthetic and in industrial white liquor

Studies of steel corrosion in SWL have been extensively reported in the literature[12,14,34-35], but reports of corrosion resistance of duplex steels in industrial liquors of pulp and mill industry are not available.

The cyclic polarization curves of the S31803 duplex steel and the S32304 lean duplex steel were similar in industrial WL at room temperature as shown in Figure 3. Polarization curves started at open circuit potentials in the range from -500 mV_{SCE} to -300 $mV_{SCE.}$ The current density increased slightly with potential until about -100 mV_{SCE}, was almost constant until about +100 mV_{SCE} and then increased slightly again at higher potentials. A slight but reproducible hysteresis was observed during the reverse scan for all samples. This electrochemical test was not able to distinguish differences in corrosion behavior of DSS and LDSS or any effect of the two processing conditions.

Figure 4 shows polarization curves of S31803 steel in synthetic and industrial WL. The corrosion potential of cold rolled S31803 DSS in SWL was -1.137 ± 0.005 V_{SCE} and in the real industrial WL it was -0.459 ± 0.014 V_{SCE}. Much higher values of current density were observed in the synthetic liquor. The differences in behavior indicate that testing of steels in synthetic liquor may predict a shorter life of the

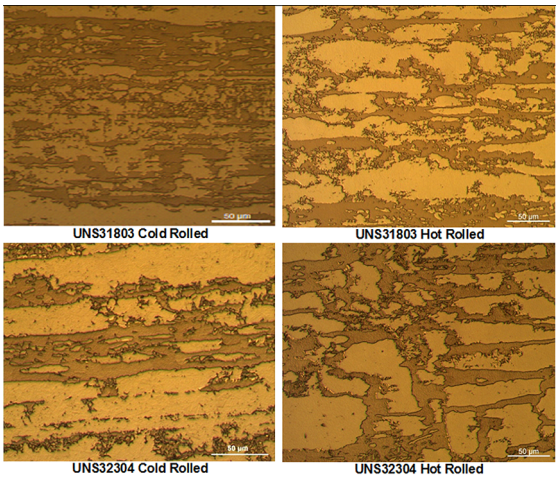

Figure 2. Microstructure of lean duplex and duplex stainless steels.

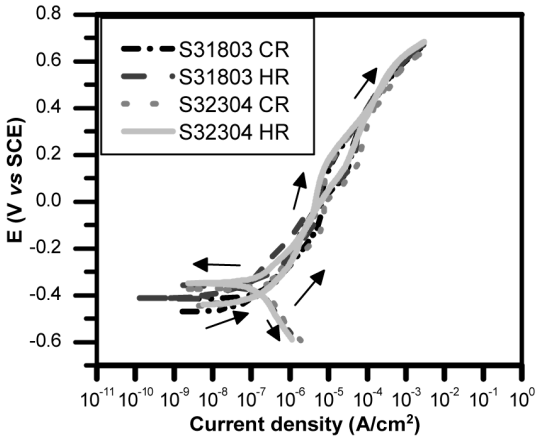

Figure 3. Cyclic polarization curves of S31803 and S32304 steels in industrial WL at room temperature.

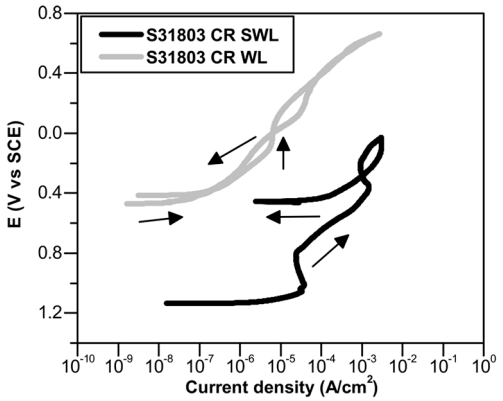

Figure 4. Cyclic potentiodynamic polarization curves for cold rolled S31803 steels in SWL and industrial WL at room temperature.

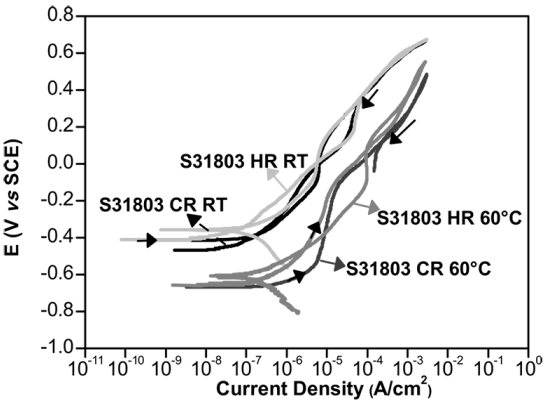

Figure 5. Cyclic potentiodynamic polarization curves of UNS 31803 DSS in industrial WLat room temperature and 60 ºC.

material than what would be achieved in service. The industrial WL is a final product from the causticizing system and it has more chemical compounds than the synthetic solution. Industrial liquors are very different from synthetic liquors, being that in the industrial process, the causticizing reactions to the formation of sodium hydroxide are reversible, which causes a variable amount of sodium carbonate to remain in the liquor. In addition, the pulp production process is cyclic, with accumulations of elements in smaller quantities coming from wood, water, and compounds present with lime. In the industrial process, it is not necessary to determine the exact chemical composition of the liquor, but rather to define an operation parameter, which is the total alkali[13,36]. The WL was regenerated in the process, as the green liquor was made caustic to produce WL, which has a complex chemical composition[27]. These extra components seem to inhibit the corrosion of DSS.

The S31803 DSS in SWLshowed two regions of almost constant current density. In contrast, in industrial WL, only one passivation region was obtained. A similar kind of behavior has been reported by Bhattacharya and Singh[14] for S32205 DSS in SWL. They suggested that the current density increased in the beginning due to the dissolution of iron, and then the primary passivation was formed by the formation of nickel sulfide (Ni_2S), with Ni and Cr also contributing to the first passivation layer[14]. The current density above the primary passivation increased due to oxidation of sulfur species corresponding to the S^{2-}/SO_4^{2-} oxidation reaction, and to the dissolution of Cr in the form of CrO_4^{2-} ions. A region of constant current density of 10^{-3}A/cm^2 was observed. Finally, the current density increased due to the oxygen evolution reaction[22]. It is reasonable to assume that this explanation is also valid for the results obtained in this study.

The corrosion potential of DSS in industrial WL at 60 ºC was less noble than the value at room temperature (RT) as shown in Figure 5, which presents the cyclic potentiodynamic polarization curves of cold and hot rolled S31803 DSS at the two temperatures. The passive current density was higher at 60 ºC (10^{-5} A/cm^2) than at RT (10^{-6} A/cm^2), indicating a less protective passive film in sulfide-containing caustic solution at the higher temperature. At about -150 mV_{SCE} for each alloy at 60 ºC, the current density increased above 10^{-5} A/cm^2. Temperature plays an important role in corrosion of duplex steels in WL and causes an increase of current densities and a decrease of open circuit potential.

3.3 Cyclic polarization of S31803, S32304 DSS in green liquor

The polarization curves of the DSSs tested in GL containing sodium carbonate and sodium sulfide at pH > 10 indicate a similar behavior for the lean and duplex stainless steels as shown in Figure 6. Two passivation regions were identified with the first one exhibiting a range of current densities between 10^{-6} to 10^{-5} A/cm^2. The duplex and lean stainless steels showed positive hysteresis in the reverse scans indicating a possibility of localized corrosion. SEM and EDS analyses identified inclusions enriched in aluminum, magnesium, oxygen, manganese and sulfur on the surface of steels. It has been reported that MgO, Al_2O_3 and MnS inclusions on the surface of S32750 super duplex steel are the preferred sites for pit initiation[31]. In this case, pits were not observed on the surface steels but these inclusions are cathodic regions and the steel near inclusions can act as anodes (Figure 7). Figure 6 shows repassivation occurring at a lower potential. Corrosion behavior of the standard duplex S31803 steel and lean duplex steel was similar in GL.

The behavior of platinum was compared with the DSS in these electrolytes as shown in Figure 6. The current densities associated with platinum are higher than the current densities exhibited by DSS, indicating that platinum surface acts as a catalyst for the redox reactions. On the other hand, the results of the DSSs were completely different from that of the platinum, and a corrosive process occurred on the surface of DSS as shown in Figure 6.

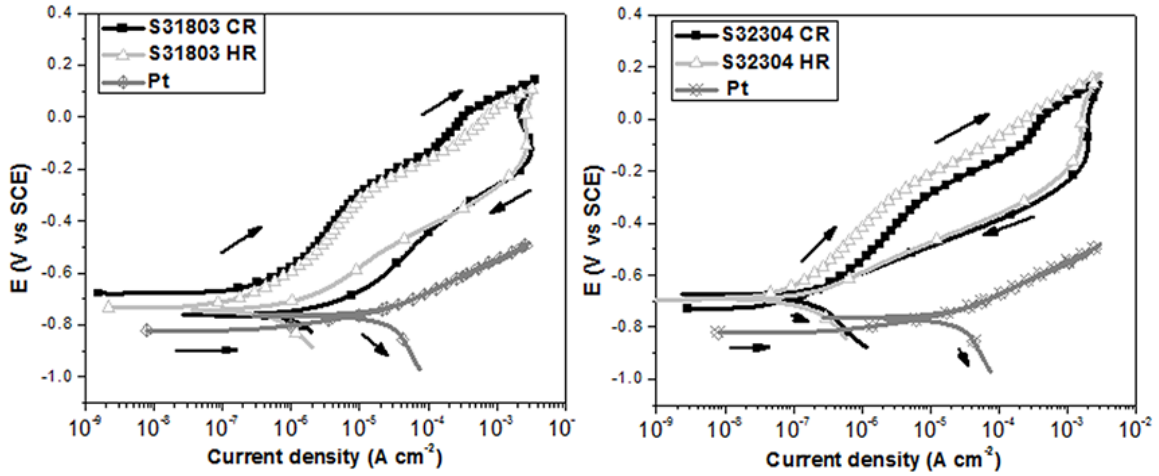

Figure 6. Cyclic potentiodynamic polarization curves of cold and hot rolled S31803 and S32304 steels, and Pt wire in green liquor at room temperature.

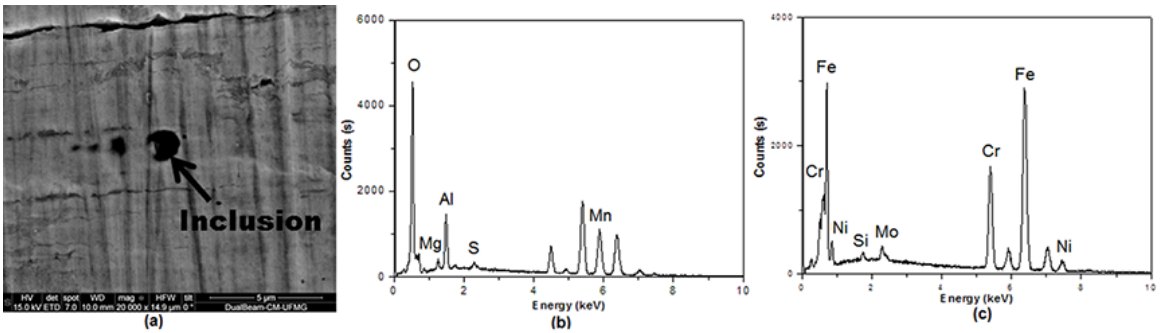

Figure 7. DSS surfaces after cyclic potentiodynamic polarization in GL: (a) 31803 CR, EDS analysis (b) inclusion spot, and (c) steel surface.

Potentiostatic polarization was performed to evaluate the behavior of the current density with time and thus the efficiency of the protective layer in GL. Three regions were chosen for the potentiostatic tests: -500 mV_{SCE} at the first passivation (around 10^{-6} A/cm^2), -150 mV_{SCE} at second passivation (around 10^{-5} A/cm^2), and 0 mV_{SCE} in the transpassive region.

The potential of -0.5 V_{SCE} was chosen to investigate the first passivation region showed in Figure 6. At the applied potential of -0.5 V_{SCE}, the current density remained constant and low with time for the steels in the cold-rolled condition and showed a slight increasing trend for the steels in the hot-rolled condition as shown in Figure 8. The cold rolled steels showed the lowest current density in green liquor. The hot rolled S31803 steel showed the highest current density in green liquor, using the potentiostatic test. The cold and hot rolled steels were annealed at 1070 ºC and 1075 ºC, respectively. In the cold rolled steel, the microstructure is finer as shown in Figure 9. The hot-rolled S31803 steel showed a passivation current density one order of magnitude higher (10^{-5} A/cm^2) than the current of the cold rolled S31803, and cold and hot rolled S32304 steels (10^{-6} A/cm^2). The hot-rolled S31803 steel exhibited a less protective layer than the other DSSs in GL.

In order to reveal the grain boundaries in austenite and ferrite in DSS, electrolytic etching was used with 60% HNO_3 solution at an etching potential of 2.2 V for 3 minutes. The cold rolled steels exhibited finer grains than the hot rolled steels (Figure 9). This finding can explain a higher tensile strength of the cold rolled steels than the hot rolled steels as shown in Table 2. Grain boundaries are barriers to the movement of dislocations and steels with finest grains have a higher density of grain boundaries that inhibits the dislocation movement and contributes to enhance the tensile strength of steel. The result obtained that the hot-rolled S31803 steel exhibited a less protective layer than the other DSSs in GL can also be explained by the lower density of grain boundaries in hot rolled S31803 steel than the steel in cold rolled condition. Finer grains contribute to improve the protective ability of the passive layer of stainless steels[37].

Cyclic polarization curves (Figure6) showed a possible second passivation region at current density of 10^{-4} A/cm^2. At the applied potential of -150 mV_{SCE}, the current density remained almost constant for the hot-rolled S31803 and the cold-rolled S32304 steels (Figure 10). The second passivation layer of hot-rolled S32304 and cold-rolled S31803 was less protective than the layer of the hot-rolled S31803 and cold rolled S32304.

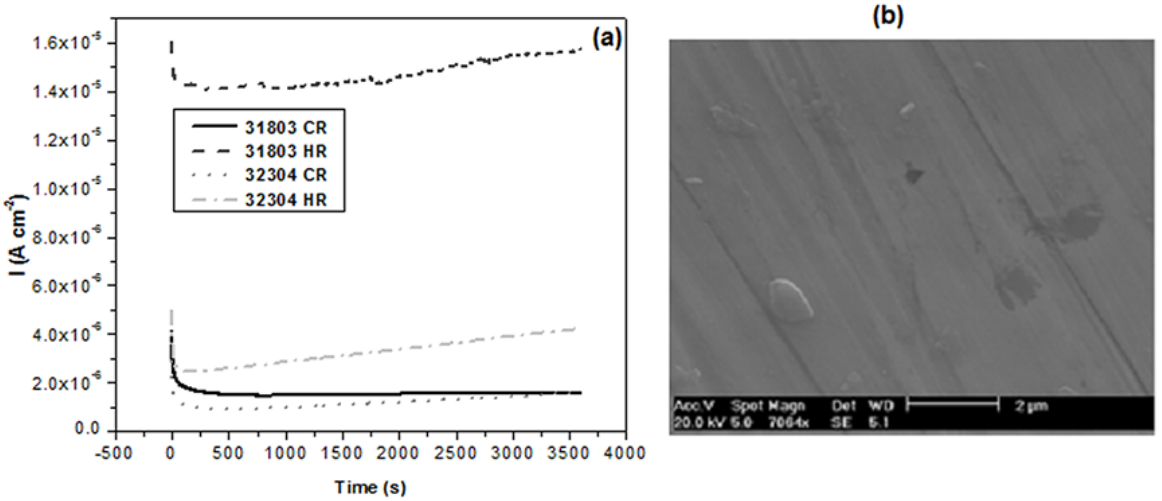

Figure 8. (a) Potentiostatic curves at -500 mV_{SCE} of cold and hot rolled S31803 and S32304 steels in green liquor at room temperature, (b) S31803 cold rolled surface after potentiostatic test at -500 mV_{SCE}.

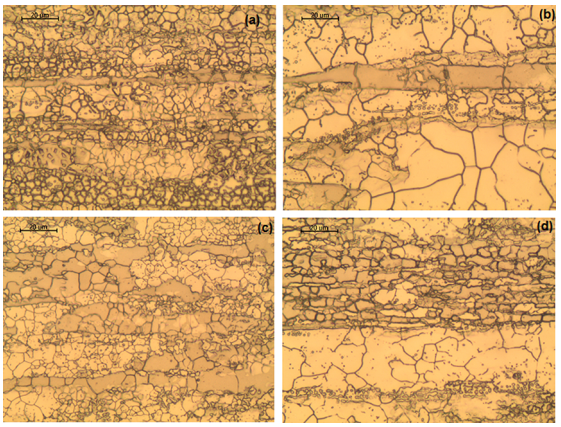

Figure 9. Grain boundaries of lean duplex and duplex stainless steels. (a) S31803 CR, (b) S31803 HR, (c) S32304 CR, and (d) S32304 HR.

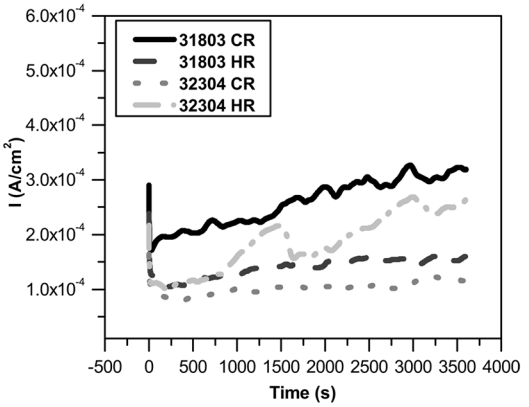

Figure 10. Potentiostatic curves at -150 mV_{SCE} of cold and hot rolled S31803 and S32304 steels in green liquor at room temperature.

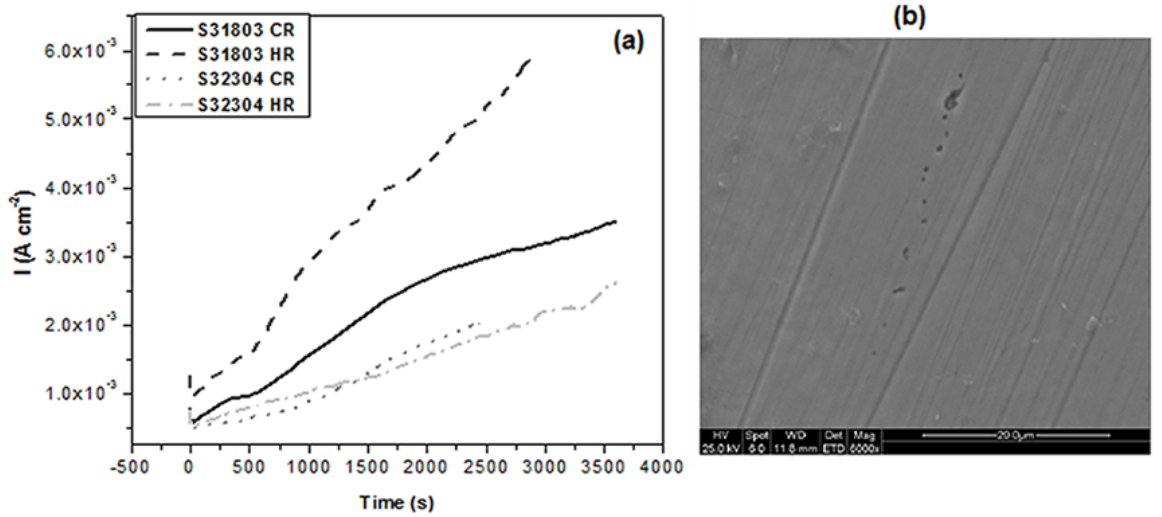

Figure 11. (a) Potentiostatic curves at 0 mV_{SCE} of cold and hot rolled S31803 and S32304 steels in GL at room temperature, (b) 32304 Cold Rolled surface after potentiostatic test at 0 mV_{SCE}.

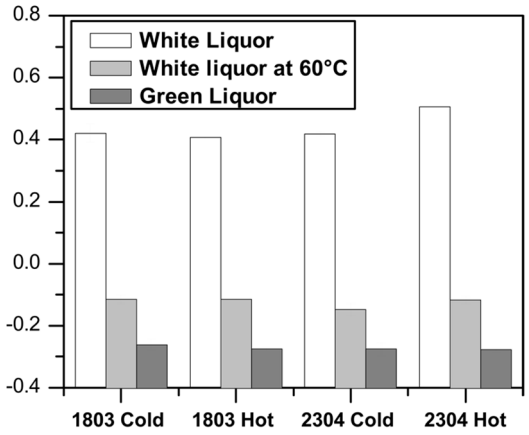

Figure 12. Average of the transpassive potential for all duplex stainless steels in industrial white, greenliquors.

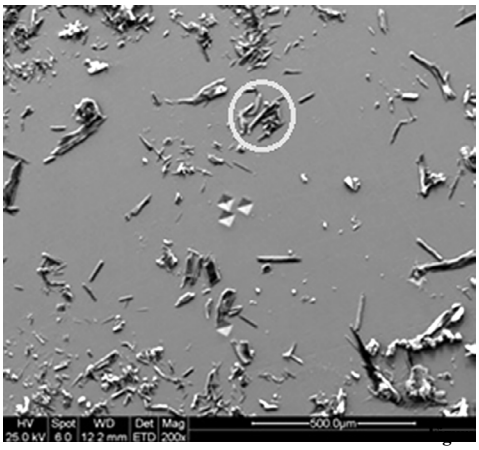

13. SEM micrographs after the cyclic potentiodynamic polarization showing carbonate precipitates on the hot 31803 duplex in green liquor.

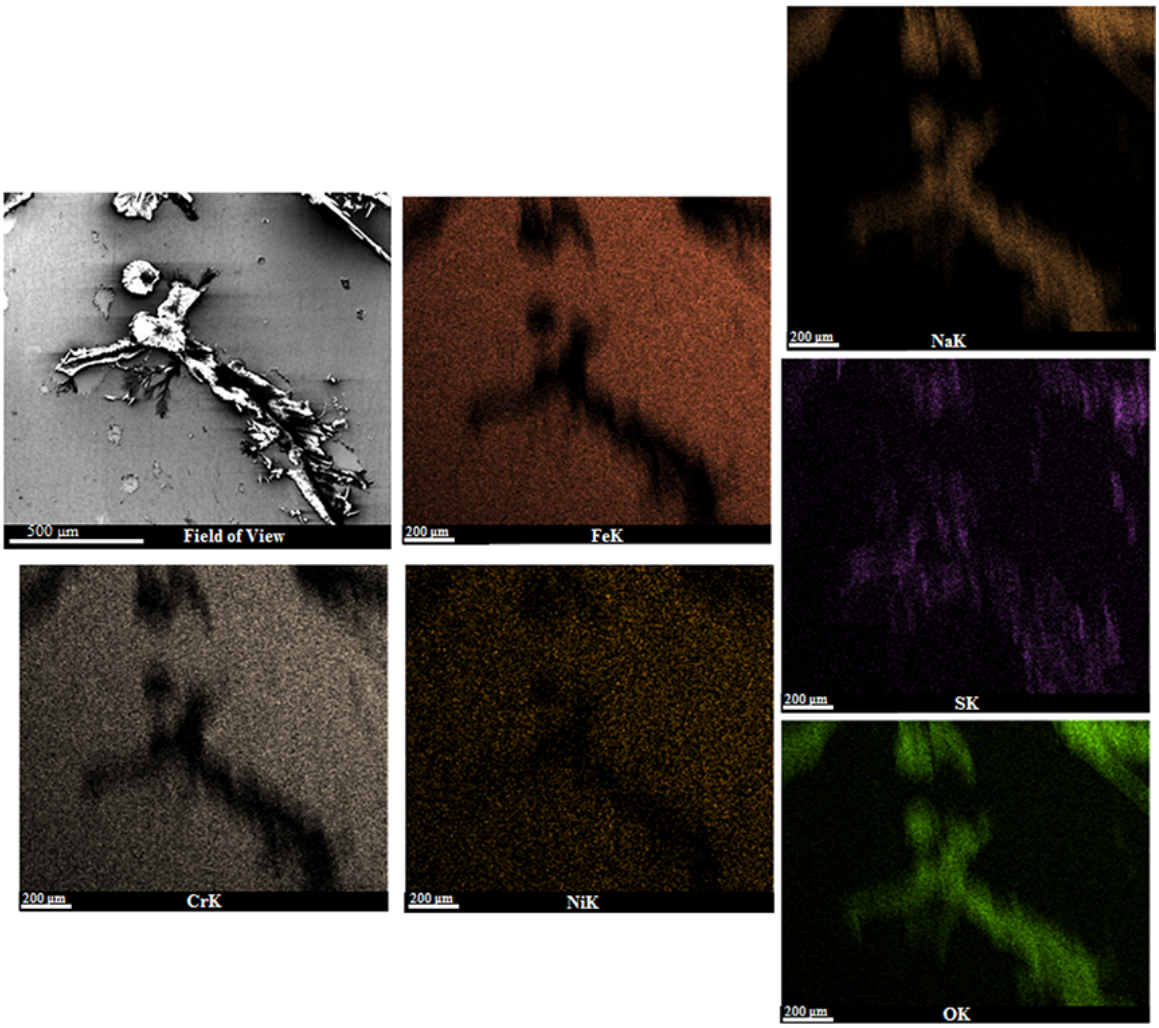

Figure 14. SEM micrographs after the cyclic potentiodynamic polarization showing carbonate precipitates on the hot 31803 duplex in green liquor.

As is evident in Figure 11, the current density increased with time when the potential of 0 mV_{SCE} was applied for all steels studied, which indicates that a corrosive process occurs at a current density on the order of 10^{-3} A/cm^2.

Temperature plays an important role for steel corrosion in WL by decreasing the transpassive potential as temperature increases (Figure 12). The WL was the less aggressive liquor for the duplex steels, which showed the highest values of transpassive potential in this medium.

In addition, cold and hot rolled duplex and lean duplex steels in green liquor showed the lowest values of transpassive potential.

Considering the passivation current density as a parameter to evaluate the corrosion behavior of steels, the GL was the most aggressive medium. It is well known that WL is more aggressive liquor due to the alkalinity[14,38]. But, in this work, the sulfide precipitation (Figure 13) plays the main role in the corrosive process, increasing corrosion, and decreasing the transpassive potential. As shown in Figure 14, the precipitate was not corrosion product of the steel due to the absence of Fe, Cr, and Ni in its chemical composition. Sodium, sulfur, and oxygen were found in the chemical composition of the precipitate, which is probably a sulfide[11].

4. Conclusions

The polarization curves of the S31803 steels in SWL were shifted to lower potentials and higher current densities in relation to the steel in industrial WL, which proved to be less aggressive to the duplex steel.

The average of transpassive potential showed that temperature plays an important role for DSS corrosion in WL decreasing the $E_{Transpassive}$ as temperature increases.

WL was the less aggressive liquor for the duplex steels, which showed the highest values of transpassive potential in this medium.

Cold and hot rolled duplex and lean duplex steels in green liquor showed the lowest values of transpassive potential.

5. Acknowledgements

The authors are grateful to the Brazilian government agencies (National Counsel of Technological and Scientific Development, Coordenação de Aperfeiçoamento de Pessoal de Nível Superior, and Fundação de Amparo à Pesquisa do Estado de Minas Gerais) for the financial support for this research.

Symbols used. $E_{Transpassive}$ [mV_{SCE}] transpassive potential

Greek letters	
γ	austenite
α	ferrite

Abbreviations

DSS	duplex stainless steel
LDSS	lean duplex stainless steel
WL	white liquor
GL	green liquor
EA	effective alkali
TTA	total titratable alkali
SCE	standard calomel electrode
SWL	synthetic white liquor
RT	room temperature
EDS	energy dispersive X-ray spectroscopy

6. References

1. Bajpai P. *Biotechnology for Pulp and Paper Processing*. New York: Springer US; 2012.
2. Bajpai P. *Chemistry and Sustainability in Pulp and Paper Industry*. Cham: Springer International; 2015.
3. Russel EH. Near-infrared spectroscopy for on-line analysis of white and green liquors. *Tappi Journal*. 1999;82(9):101-106.
4. Hazlewood PE, Singh PM, Hsieh JS. Effect of Black Liquor Oxidation on the Stress Corrosion Cracking Susceptibility of Selected Materials. *Corrosion Science*. 2006;62(9):765-772.
5. Kent JA, ed. *Handbook of Industrial Chemistry and Biotechnology*. New York: Springer US; 2012. p. 218-222.
6. Demirbas A. Pyrolysis and steam gasification processes of black liquor. *Energy Conversion and Management*. 2002;43(7):877-884.
7. Wensley A. Corrosion and Cracking of Bottom Scrapers in Continuous Digesters. In: *Corrosion 2005*; 2005 Apr 3-7; Houston, TX, USA. NACE-05199.
8. Kannan S, Kelly RG. The role of dihydroxybenzenes and oxygen on the corrosion of steel in black liquor. *Corrosion Science*. 1996;38(7):1051-1069.
9. Bajpai P. *Chemical Recovery in Pulp and Papermaking*. Surrey: Pira International; 2008. 166 p.
10. Kinnarinen T, Golmaei M, Jernström E, Häkkinen A. Separation, treatment and utilization of inorganic residues of chemical pulp mills. *Journal of Cleaner Production*. 2016;133:953-964.
11. Manskinen K, Nurmesniemi H, Pöykiö R. Total and extractable non-process elements in green liquor dregs from the chemical recovery circuit of a semi-chemical pulp mill. *Chemical Engineering Journal*. 2011;166(3):954-961.
12. Tuthill AH, ed. *Stainless Steels and Specialty Alloys for Modern Pulp and Paper Mills*. Toronto: Nickel Development Institute (NiDI); 2002.
13. Cardoso M, de Oliveira ED, Passos ML. Chemical composition and physical properties of black liquors and their effects on liquor recovery operation in Brazilian pulp mills. *Fuel*. 2009;88(4):756-763.
14. Bhattacharya A, Singh PM. Electrochemical behaviour of duplex stainless steels in caustic environment. *Corrosion Science*. 2011;53(1):71-81.

15. Outokumpu. *Activating Your Ideas - Stainless Steel for Pulp & Paper Processes*; 2008. Available from: <https://www.outokumpu.com/SiteCollectionDocuments/Stainless_for_desalination_brochure.pdf>. Access in: 20/11/2017.

16. Jiang D, Ge C, Zhao X, Li J, Shi L, Xiao X. 22Cr High-Mn-N Low-Ni Economical Duplex Stainless Steels. *Journal of Iron and Steel Research, International*. 2012;19(2):50-56.

17. Wensley A. Pulp and Paper. In: Baboian R, ed. *Corrosion Tests and Standards: Application and Interpretation*. 2nd ed. West Conshohocken: ASTM International; 2005. p. 795-811.

18. Wensley A. Corrosion Protection of Kraft Digesters. In: *Corrosion 2001*; 2001 Mar 11-16; Houston, TX, USA. NACE-01423.

19. Paoliello F, Lins VFC, Cardoso M. Influence of cooking conditions on continuous digester corrosion in a Brazilian pulp mill. *Tappi Journal*. 2011;10:51-60.

20. Chater BJ. The pulp and paper industry turns to duplex. *Stainless Steel World*. 2007;3:70-77.

21. Munro I. Anodic Protection of Continuous Digesters to Prevent Corrosion and Cracking. *Proceedings of TAPPI Engineering Conference*. 1983;13303:181-185.

22. Singh PM, Anaya A. Effect of wood species on corrosion behavior of carbon steel and stainless steels in black liquors. *Corrosion Science*. 2007;49(2):497-509.

23. Wensley A. Corrosion in Alkaline Pulping Liquors. In: *Corrosion 2004*; 2004 Mar 28-Apr 1; New Orleans, LA, USA; 2004. NACE-04248.

24. Wang Y, Singh P. Corrosion Behavior of Austenitic and Duplex Stainless Steels in Thiosulfate and Chloride Containing Environments. *Corrosion*. 2015;71(8):937-944.

25. Bhattacharya A, Singh PM. Effect of Heat Treatment on Corrosion and Stress Corrosion Cracking of S32205 Duplex Stainless Steel in Caustic Solution. *Metallurgical and Materials Transactions A*. 2009;40(6):1388-1399.

26. Wensley A, Champagne P. Effect of Sulfidity on the Corrosivity of White, Green, and Black Liquors. In: *Corrosion 1999*; 1999 Apr 25-30; San Antonio, TX, USA; NACE-99281.

27. Sharma A, Sharma S, Sharma S. In Plant Test for Corrosion Investigations in Digester of a Paper Mill. *Journal of Materials and Environmental Science*. 2013;4(3):420-425.

28. APERAM Stainless Steel Europe. *DX2304*; 2017. Available from: <http://www.aperam.com/uploads/stainlesseurope/TechnicalDataSheet/FT Duplex/Anglais/FT_DX2304_UK.pdf>. Access in: 27/11/2017.

29. Magnabosco R. Kinetics of sigma phase formation in a Duplex Stainless Steel. *Materials Research*. 2009;12(3):321-327.

30. Frankel GS, Dukovic JO, Brusic V, Rush BM, Jahnes CV. Pit Growth in NiFe Thin Films. *Journal of the Electrochemical Society*. 1992;139(8):2196-2201.

31. Feng H, Li H, Zhang S, Wang Q, Jiang Z, Li G, et al. Corrosion Behavior of Super Duplex Stainless Steel S32750 in White Liquor. *International Journal of Electrochemical Science*. 2015;10:4116-4128.

32. Michalska J, Sozańska M. Qualitative and quantitative analysis of σ and χ phases in 2205 duplex stainless steel. *Materials Characterization*. 2006;56(4-5):355-362.

33. Jimenez JA, Carsi M, Ruano OA, Peñalba F. Characterization of a δ/γ duplex stainless steel. *Journal of Materials Science*. 2000;35(4):907-915.

34. Crowe DC. Stress Corrosion Cracking of Carbon Steel in Kraft Digester Liquors. In: *6th International Conference on Corrosion in the Pulp and Paper Industry*. 1989 Aug 29-Sep 1; Helsinki, Finland.

35. Peterman L, Yeske RA. *Thiosulfate Effects on Corrosion in Kraft White Liquor*. Appleton: IPC Technical Paper Series; 1986.

36. Green RP, Hough G. *Chemical Recovery in the Alkaline Pulping Processes*. Atlanta: TAPPI Press; 1992.

37. Zheng ZJ, Gao Y, Gui Y, Zhu M. Corrosion behaviour of nanocrystalline 304 stainless steel prepared by equal channel angular pressing. *Corrosion Science*. 2012;54:60-67.

38. Singh PM, Ige O, Mahmood J. Stress Corrosion Cracking of Type 304L Stainless Steel in Sodium Sulfide-Containing Caustic Solutions. *Corrosion*. 2003;59(10):843-850.